ACS APPLIED MATERIALS & INTERFACES

Research Article

www.acsami.org

Synthesis of Hierarchical Micro/Mesoporous Structures via Solid–Aqueous Interface Growth: Zeolitic Imidazolate Framework-8 on Siliceous Mesocellular Foams for Enhanced Pervaporation of Water/Ethanol Mixtures

Yu-Chain Sue,[†] Jhe-Wei Wu,[†] Shao-En Chung,[†] Chao-Hsiang Kang,[‡] Kuo-Lun Tung,[‡] Kevin C.-W. Wu,*[,‡] and Fa-Kuen Shieh*[,†]

[†]Department of Chemistry, National Central University, 300 Jhong-Da Road, Chung-Li 32001, Taiwan

[‡]Department of Chemical Engineering, National Taiwan University, No. 1, Sec. 4, Roosevelt Road, Taipei 10617, Taiwan

Supporting Information

ABSTRACT: A new hierarchical micro/mesoporous composite is synthesized via direct growth of microporous zeolitic imidazolate framework-8 (ZIF-8) on siliceous mesocellular foams (MCF). Depending on different synthetic conditions, ZIF-8 with two different particle sizes, i.e., ZIF-8 microparticles and ZIF-8 nanoparticles, were successfully formed on the external surface of amine-functionalized MCF (denoted as microZIF-8@MCF and nanoZIF-8@MCF, respectively). The synthesized hierarchical micro/mesoporous ZIF-8@MCF structures were characterized with several spectroscopic techniques including X-ray diffraction (XRD), solid-state NMR, and FT-IR and electron microscopic techniques (scanning electron microscope, SEM, and transmission electron microscopy, TEM). In addition, the pervaporation measurements of the liquid water/ethanol mixture show that nanoZIF-8@MCF/PVA (poly(vinyl alcohol) mixed-matrix membrane exhibits enhanced performance both on the permeability and separation factor. Compared to conventional routes for chemical etching, this study demonstrates a promising and simple strategy for synthesizing novel hierarchical porous composites exhibiting both advantages of mesoporous materials and microporous materials, which is expected to be useful for gas adsorption, separation, and catalysis.

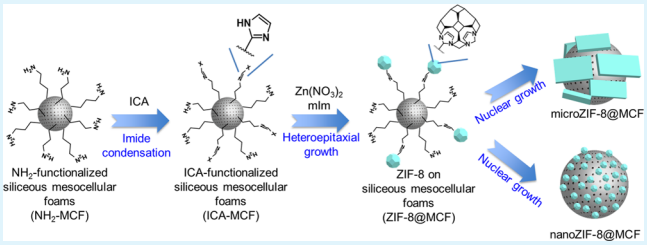

KEYWORDS: *hierarchical structures, zeolitic imidazolate framework, mesoporous silica, pervaporation, separation factor*

1. INTRODUCTION

Porous materials[1] are being used in a wide range of industrial and biological processes such as catalysis[2−4] and adsorption/separation[5] owing to their high surface area and unique pore size, which when coupled with their distinctive surface chemistry offer the possibility of size and shape selective reactions. Porous materials are typically classified according to their pore sizes.[6] In general, three categories have been defined: pores in the size range of 2 nm and below are called micropores; those in the size range of 2−50 nm are denoted as mesopores; and those above 50 nm are categorized as macropores. The distribution of size, shape, and volume of the void spaces in porous materials could be directly related to their ability to perform the desired function in a particular application.[7,8] For example, a material with uniform micropores, such as a zeolitic imidazolate framework (ZIF),[9−12] can separate molecules on the basis of their size by selectively adsorbing molecules smaller than its pores from a mixture predominantly containing molecules larger to enter its pores. Thus, the pore size distribution in the material clearly limits the ability of a solid to separate molecules of different sizes.

Very recently, ZIF-based mixed matrix membranes have been demonstrated to be promising for pervaporation technology. For example, the Chung group has reported the synthesis of ZIF-8/polybenzimidazole (PBI) mixed-matrix membranes for pervaporation dehydration of alcohols.[13] The Yang group reports the ZIF-8/polymethylphenylsiloxane (PMPS) for both pervaporation and vapor permeation of furfural.[14] Another hydrophobic ZIF material (ZIF-71) was incorporated into polyether-block-amide (PEBA) polymer for recovery of biobutanol.[15] We also previously synthesized ZIF-7/chitosan mixed-matrix membranes for separation of water/ethanol mixtures.[16] These pioneering studies all demonstrated that the introduction of microporous and inorganic ZIF materials into organic polymers could greatly improve the permeability, mechanical toughness, and selectivity of the fabricated ZIF-based mixed-matrix membranes.

In many cases, however, a combination of two materials with different pore sizes can exhibit properties superior to those of

Received: January 23, 2014
Accepted: March 13, 2014
Published: March 13, 2014

   dx.doi.org/10.1021/am5004188 | ACS Appl. Mater. Interfaces 2014, 6, 5192−5198

the individual constituents.[17] Such a combination of pore sizes spanning different length scales is referred to as hierarchical structuring. Recently, hierarchical structuring[18−26] of zeolitic materials has emerged as an area of significant scientific interest because of its potential technological impact in adsorption/separation, catalysis, microelectronics, biomolecular separation, and chromatographic applications.[27−29] This type of structuring combines the benefits of each pore-size regime in addition to providing inherent advantages such as different length scales and superior mass/heat transfer characteristics, irrespective of whether the constituent networks are ordered or disordered.[30]

In this study, we have synthesized novel hybridized particles with hierarchical structure through direct coating of microporous ZIF-8 particles onto siliceous mesocellular foams (MCF), as shown in Scheme 1. MCF was first synthesized

Scheme 1. Schematic Illustration of the Synthetic Process for Hierarchical Micro/Mesoporous ZIF-8@MCF Materials

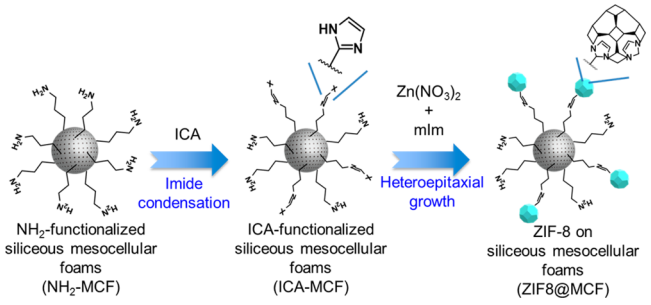

through a phase transition of a highly ordered mesoporous silica SBA-15. The surface of MCF was then functionalized with amine groups (denoted as NH_2-MCF). After that, imidazole-2-carboxaldehyde (ICA) was added and reacted with NH_2-MCF through imide condensation (denoted as ICA-MCF). Finally, $Zn(NO_3)_2$ and 2-methylimidazole (mIm) were added and resulted in the formation of ZIF-8 on the surface of ICA-MCF through direct growth (denoted as ZIF-8@MCF). Compared to the type of mesoporous silica SBA-15, MCF possessed remarkable mesostructured cellular foams composed of uniformly sized and large spherical cells,[31] so they are more appropriate for direct growth of microporous materials.

2. MATERIALS AND METHODS

2.1. Chemicals. The templating agent Pluronic P123, zinc nitrate hexahydrate, PVA (poly(vinyl alcohol) average MW 146,000−186,000, 99+% hydrolyzed), and glutaraldehyde (GA, 50 wt % aqueous solution) were purchased from Sigma-Aldrich. 3-Aminopropyl-triethoxysilane (APTS) and 2-methylimidazole (mIm) were obtained from ACROS. Tetraethoxysilane (TEOS) and 1,3,5-trimethylbenzene (TMB) were acquired from Fluka and Grand, respectively. Sulfuric acid (H_2SO_4) was purchased from Merck. Hydrochloric acid (HCl) and ammonium fluoride (NH_4F) were purchased from Riedel-Dehean and SHOWA, respectively. Imidazole-2-carboxaldehyde (ICA) and *N*,*N*-dimethyl-formamide (DMF) were purchased from Alfa Aesar and EMPARTA, respectively. All chemicals were used without further purification.

2.2. Synthesis of ZIF-8@MCF. The MCF sample was initially prepared by the method described in the literature.[32−34] For functionalization of MCF with NH_2 groups, 0.60 g of MCF was added to 2.5 mL (0.01 mmol) of 3-aminopropyl-triethoxysilane prepared in ethanol (10 mL). The reaction mixture was stirred for 40 h. Precipitates thus obtained were filtered, washed with excess ethanol, and vacuum-dried at 100 °C overnight (denoted hereafter as NH_2-MCF). Subsequently, 85 mg (0.89 mmol) of imidazolate-2-carboxyaldehyde (ICA) was added to 100 mg of NH_2-MCF to link ICA to the NH_2 groups of NH_2-MCF, and the resulting sample was designated as ICA-MCF.[35] Then, 100 mg of dried ICA-MCF was mixed with 146 mg (1.78 mmol) of 2-methyl-imidazolate (mIm) in DMF (30 mL). This reaction mixture was stirred for 24 h, added with 582 mg (1.95 mmol) zinc nitrate hexahydrate ($Zn(NO_3)_2{\cdot}6H_2O$), and again stirred for at least 5 min at room temperature to get a homogeneous solution. The mixed solution was then placed in an oven and maintained at 140 °C for 24 h. The incubated solution was cooled down to ambient conditions and filtered to separate the precipitate from DMF. To obtain the final product, the filtered precipitate was added with chloroform (10 mL) and centrifuged for suspending the particles of ZIF-8 in the mixture on account of the difference in density;[36] the same process was repeated at least three times. The precipitant thus obtained was filtered, washed with excess methanol, and vacuum-dried at 100 °C overnight (represented as microZIF-8@MCF). To synthesize nanoscale ZIF-8, we modified a previous report where the mole ratio of mIm/zinc salt was maintained at 70.[37] Typically, 100 mg of dried ICA-MCF was mixed with 11.35 g (138.5 mmol) of mIm in 40 g of DI water and then stirred for 1 h (solution A). Then, 585 mg (1.96 mmol) of zinc nitrate hexahydrate was prepared in 4 g of DI water and used as a triggered solution (solution B). After mixing of solutions A and B at room temperature for 30 min, a powder appeared and was collected by centrifugation. In order to obtain the final product, powdered resultants was added with chloroform (10 mL) and centrifuged for suspending the particles of ZIF-8 in the mixture on account of the difference in density.[36] The precipitant thus obtained was vacuum-dried at 60 °C overnight (represented as nanoZIF-8@MCF).

2.3. Preparation of ZIF-8@MCF/PVA Mixed-Matrix Membranes. PVA powders were first dissolved in deionized water to form a PVA solution with concentration of 5 wt %. The solution was subsequently separated using a filter paper (pore size of 6 μm) to remove impurities. Then, nanoZIF-8@MCF particles were added into the PVA solution under ultrasonication for 1 min. The ratio of nanoZIF-8@MCF to PVA was fixed at 0.05 (in weight). The whole solution (i.e., casting solution) was then reacted with glutaraldehyde for 30 min in order to cross-link PVA polymer. Finally, this casting solution was carefully poured onto the glass plate and was cast to form a film (i.e., mixed-matrix membrane). The nanoZIF-8@MCF/PVA membrane was slowly dried in an oven at 45 °C overnight and then could be peeled from the glass plate. A pristine PVA membrane was also prepared using the same process for comparison.

2.4. Pervaporation Measurements. The mixture of ethanol (90 wt %) and water was separated through the ZIF-8@MCF/PVA membranes using a published pervaporation process at a feed temperature of 25 °C.[38] The pressure of the permeate was controlled at 3−5 mmHg, and the temperature was controlled at 25 °C by using a thermostatic water bath. The flux and composition of permeate were analyzed by measuring the permeate weight with a gas chromatography (GC-4000, GL Sciences, Japan). The separation factor (i.e., $\alpha_{water/EtOH}$) was calculated according to the following equation:

$$\alpha_{water/EtOH} = \frac{Y_{water}/Y_{EtOH}}{X_{water}/X_{EtOH}}$$

where X_{water} and X_{EtOH} are the weight fractions of water and ethanol, respectively, in the feed solution, and Y_{water} and Y_{EtOH} are the weight fractions of water and ethanol, respectively, in the permeate.

2.5. Characterization. Powder X-ray diffraction (XRD) patterns were collected by PANalytical X'Pert PRO. N_2 adsorption/desorption isotherms were measured at 77 K on a Micromeritics ASAP 2020 analyzer. The samples were degassed at 95 °C for 24 h before the measurements. Specific surface areas were calculated by using the Brunauer−Emmett−Teller (BET) method in the relative pressure range of P/P_0 = 0.05−0.30. Pore volumes were obtained from the volumes of N_2 adsorbed at P/P_0 = 0.95 or in the vicinity. Fourier transform infrared (FTIR) spectra of the samples were recorded at room temperature on a JASCO FT/IR-4100. Each sample was scanned 20 times at 4 cm^{-1} resolution over the range of 4000−400

dx.doi.org/10.1021/am5004188 | ACS Appl. Mater. Interfaces 2014, 6, 5192−5198

cm^{-1}. Solid-state ^{13}C CP/MAS NMR spectra were recorded by using a contact time of 3 ms on a Varian Infinityplus-500 NMR spectrometer, equipped with a 5.0 mm Chemagnetics probe. The Larmor frequency for the ^{13}C nucleus was 125.7 MHz. The ^{13}C chemical shift was externally referenced to tetramethylsilane (TMS) at 0 ppm. Field-emission scanning electron microscope (FESEM) images were taken by using a JEOL JSM-7000, and the acceleration voltage was 15 kV. High resolution scanning transmission electron microscopy (HR-STEM) images was taken with JEM-2100 equipped with an Oxford inca energy 250-dispersive X-ray spectroscopy system. Thermal gravimetric analysis (TGA) measurements were performed on a METTLER SDTA851. Samples (approximately 2 mg) were filled into an alumina crucible and heated in a continuous-flow of nitrogen gas with a ramp rate of 10 °C min^{-1} from 25 up to 1000 °C.

3. RESULTS AND DISCUSSION

The structural properties of the as-synthesized ZIF-8@MCF materials were analyzed using X-ray powder diffraction (XRD). As shown in Figure 1a, the diffraction pattern of the parent

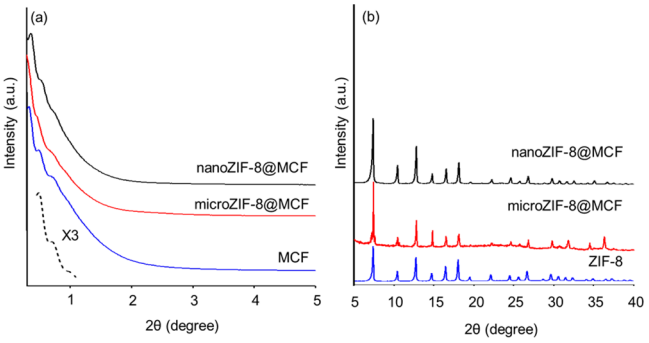

Figure 1. (a) Small-angle and (b) large-angle XRD patterns for MCF, microZIF-8@MCF, nanoZIF-8@MCF, and ZIF-8 materials.

MCF material showed three weak shoulder-like peaks in the region 2θ = 0.7−2.0° that could be associated with the characteristic peaks of 3D mesostructured cellular foams exhibiting uniform and large spherical pores (around 15 nm).[31] These structural features remained well for ZIF-8@MCF, indicating that the ZIF-8 materials did not occupy the mesopores of MCF and were indeed produced from the external surface of MCF through in situ growth. In addition to small-angle XRD patterns, the large-angle XRD patterns in Figure 1b showed that the final ZIF-8@MCF composites (i.e., microZIF-8@MCF and nanoZIF-8@MCF) exhibited characteristic crystalline peaks of conventional ZIF-8.[36,37] These XRD patterns confirm the coexistence of hierarchical structures (i.e., mesostructure from MCF and microstructure from ZIF-8) in the synthesized ZIF-8@MCF composites. Remarkably, three peaks appearing at the high 2θ angle region of 31.5°, 34°, and 36° in microZIF-8@MCF patterns could be contributed by side products of ZnO particles.[39]

To investigate the in situ formation of ZIF-8 on MCF, ^{13}C cross-polarization magic-angle spinning (CP/MAS) NMR spectroscopy was employed to monitor the status of the imidazolate carbons before and after ZIF-8 formation (Figure 2 and Figure S1 (Supporting Information)). According to the ^{13}C NMR patterns, a peak corresponding to imidazolate carbon in the ICA linkage (i.e., peaks attributable to imine bond at 166.3 ppm (C4)) was observed for the ICA-MCF sample, and this peak shifted downfield after the formation of ZIF-8@MCF. In addition, the ^{13}C NMR pattern of the ICA-MCF sample showed several imidazolate carbon atom resonances between

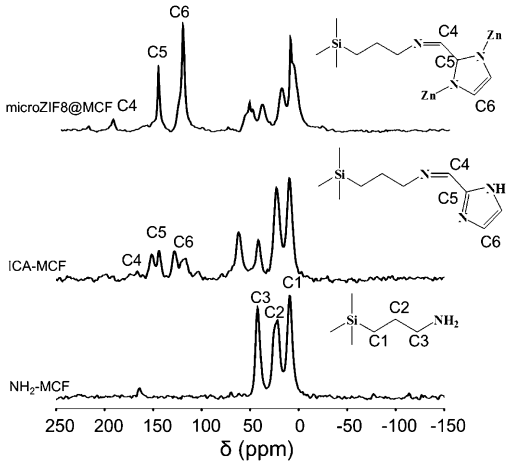

Figure 2. ^{13}C CP/MAS NMR spectra of NH_2-functionalized MCF, ICA-functionalized MCF, and microZIF-8@MCF samples.

100 and 150 ppm, and these peaks remained well for the ZIF-8@MCF sample, indicating a successful linkage of ICA and Zn ion upon ZIF-8 formation. In addition to NMR results, we also used Fourier transform infrared (FT-IR) spectroscopy to investigate the in situ formation of ZIF-8 on MCF. As shown in Figure S2 (Supporting Information), a peak at ∼1650 cm^{-1} appeared for the ICA-MCF sample, which represents the C═N bond of the imine group in ICA. After the formation of ZIF-8 on MCF, this peak became broad and its intensity decreased, indicating the electron environment on ICA changed when ICA molecules were reacted with $Zn(NO_3)_2$ and mIm to form ZIF-8. Furthermore, a comparison of the IR spectra in the fingerprint region (i.e., 500−1500 cm^{-1}) revealed the similarity in the spectra of ZIF-8@MCF and ZIF-8. The FT-IR spectra again confirm the growth of ZIF-8 on the parental MCF materials.

The porous properties of the synthesized materials were analyzed with nitrogen adsorption/desorption isotherms, and the results were displaced in Figure 3 and summarized in Table 1. As shown in Figure 3, the synthesized ICA-MCF and ZIF-8@MCF (microZIF-8@MCF) samples showed typical type-IV isotherms that are similar to that of its parent MCF material.[40,41] However, upon the functionalization of NH_2 and ICA molecules, both specific surface area and pore volume

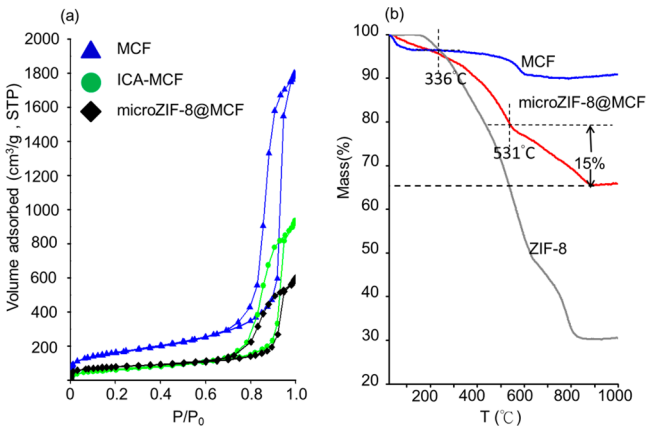

Figure 3. (a) N_2 adsorption−desorption isotherms of MCF (triangle ▲), ICA-MCF (circle ●), and microZIF-8@MCF (kite ♦). (b) TGA profile of ZIF-8, microZIF-8@MCF, and MCF.

dx.doi.org/10.1021/am5004188 | ACS Appl. Mater. Interfaces 2014, 6, 5192−5198

Table 1. Summary of Materials Synthesized in This Study

	nitrogen adsorption			
sample	S_{BET}/m^2g^{-1}[a]	V/cm^3g^{-1}[b]	window diameter/nm[c]	cell diameter/nm[d]
ZIF-8[36]	1630	0.63	3.40	11.60
MCF	592	2.80	14.70	19.88
NH_2-MCF	282	1.58	13.70	20.36
ICA-MCF	243	1.45	13.50	21.37
microZIF-8@MCF	279	0.9	13.3	18.58
nanoZIF-8@MCF	935	0.64	15.30	18.07

[a]BET surface area. [b]Total pore volume. [c]Window diameter calculated from desorption branch. [d]Cell diameter calculated from adsorption branch.[31]

decreased, indicating the occupation of NH_2-containing organosilanes and ICA molecules. After the formation of ZIF-8, the isotherm of the ZIF-8@MCF sample exhibited a small step-like feature with a flattened hysteresis and narrow loop originated at high relative pressure. This could be attributed to mesoporous properties of MCF material. It is worth noting that, in all samples, the pore diameter did not alter too much. This result confirmed that the mesoporous structure of the parent MCF remained well upon functionalization and growth of ZIF-8 (see Figures S3 and S4 in the Supporting Information).

The thermal properties of the samples were also investigated using thermogravimetric analysis (TGA). As shown in Figures 3b and Figure S5 (Supporting Information), the decomposition of ZIF-8 and the removal of guest molecules from the cavities in the microZIF-8@MCF sample proceeded gradually with a weight-loss step between approximately 25 and 340 °C corresponding to a loss of guest species and, above approximately 530 °C, the decomposition of ZIF-8 took place. Thus, it also indicates the percentage of ZIF-8 in the composite of microZIF-8@MCF is approximately 15% (w/w). Furthermore, the Figure S5 (Supporting Information) showed the TGA profile of nanoZIF-8@MCF with a deep drop curve below 180 °C due to guest species of water solvent. Because the TGA curve of the parent MCF sample did not show appreciable weight losses below 500 °C, similarly consistent with a previous report,[42] the weight loss was supposed to be the result from the postgrown ZIF-8 nanoparticles.

Depending on different synthetic conditions, ZIF-8 with two different sizes (i.e., microparticles and nanoparticles) could be successfully produced. As shown in Figure 4, the SEM images with different magnifications show that ZIF-8 synthesized in DMF system exhibited a plate-like morphology and a micrometer-scale particle size (Figure 4a-1, a-2), while another kind of ZIF-8 with a sphere-like morphology and a nanoscale particle size could be obtained at water-based synthetic conditions (Figure 4b-1,b-2).[37] Figure 4c illustrates the formation of ZIF-8 with different particle size on the parent MCF materials. In either case, it is remarkable to notice that MCF is seemingly to have been partially coated with a crystalline layer of ZIF-8. Analogously, XRD patterns shown in Figure 1a indicated that the structural integrity of parental MCF is maintained after the formation of a ZIF-8 layer. In addition, the formation of nanoZIF-8 on MCF increases the surface area, which was contributed by high-surface-area ZIF-8 particles (Table 1). It is consistent with the observation in ^{13}C NMR spectra of nanoZIF-8@MCF and ZIF-8 sharing with

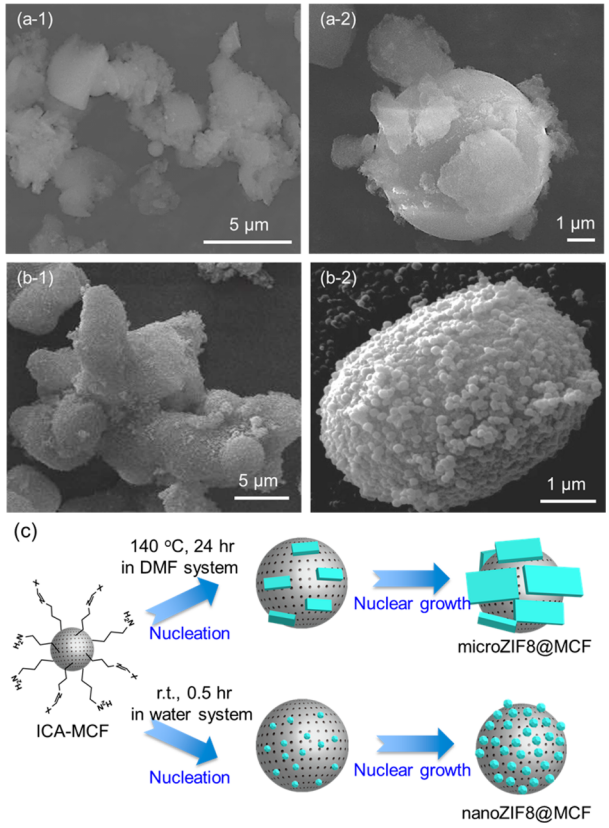

Figure 4. SEM images of ZIF-8 with (a) large and (b) small particle sizes synthesized in DMF and water systems, respectively. (a-1 and b-1 are low magnification; a-2 and b-2 are high magnification) (c) An illustration presumably expressing the synthetic processes for ZIF-8@MCF with two different kinds of ZIF-8 (plate-like microparticles and sphere-like nanoparticles). Nucleation and nuclear growth steps not snapped in SEM images.

mostly identical patterns (see Figure S1 in the Supporting Information).

The existence of the ZIF-8 layer that was indeed grown on the external surface of MCF was confirmed by transmission electron microscopy (TEM) (Figure 5a) and energy dispersive

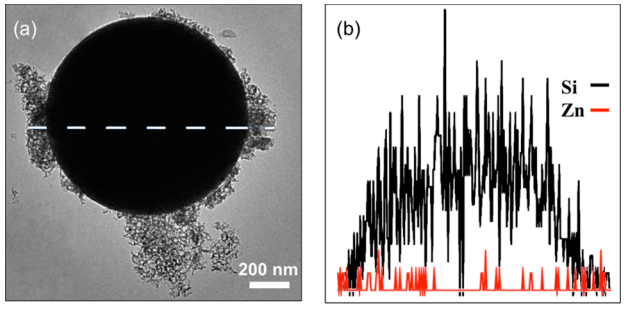

Figure 5. (a) A TEM image of microZIF-8@MCF and (b) its corresponding EDX line scanning for both Si and Zn elements.

X-ray (EDX) spectroscopy (Figure 5b). It is clear to see that Si and Zn elements that are contributed by MCF and ZIF-8 materials, respectively, appeared in Figure 5b. The EDX line scanning for the Zn and Si taken diameter lines confirms that Zn element is one of the constituents of the hybrid materials. Remarkably, the consequence of EDX line scanning also indicates that the presence of Zn across the whole diameter

dx.doi.org/10.1021/am5004188 | ACS Appl. Mater. Interfaces 2014, 6, 5192−5198

clearly demonstrates that the shell of hybrid particle is likely composed of Zn-based material. This is once again in agreement with ZIF-8 materials grown on the surface of MCF materials, resulting in a hierarchical porous structure.

In order to demonstrate the advantage of the hierarchical structure of the synthesized ZIF-8@MCF composites, the pervaporation for the separation of ethanol and water was measured with the presence of three kinds of membranes: pristine PVA membrane, MCF/PVA mixed-matrix membrane, and nanoZIF-8@MCF/PVA mixed-matrix membrane. As compared with the result of the pristine PVA membrane, the MCF-doped mixed matrix membrane showed increased flux but decreased separation factor, as shown in Figure 6. This is

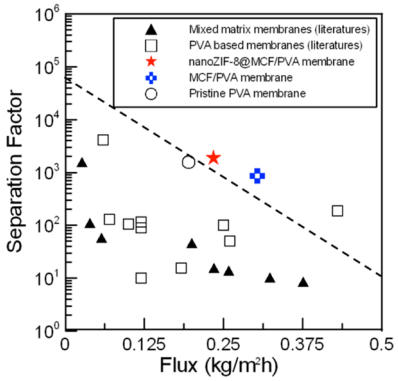

Figure 6. The pervaporation performance of nanoZIF-8@MCF-doped PVA membranes compared with results from the literature, where other PVA-based mixed-matrix membranes were used. The line is a general trend.

because MCF provides large pore volume (2.8 cm^3g^{-1}) in the MCF/PVA mixed-matrix membrane. Although the flux increased, the large pore of MCF in the membrane also reduces the performance of separation. In contrast, the nanoZIF-8@MCF-doped mixed-matrix membrane exhibited great performance both on the increased flux and separation factor. We suggest that the enhanced separation factor was the result of the presence of nanoZIF-8 because nanoZIF-8 provides a suitable pore size (i.e., 3.4 Å) that can allow smaller molecules such as water (size is 2.96 Å) to pass through but block larger molecules such as ethanol (size is 4.3 Å). In addition, the presence of MCF in the membrane can provide large pore volume, thus increasing the flux. The nanoZIF-8@MCF/PVA mixed-matrix membrane prepared in this study is superior to most PVA-based membranes,[43−51] which clearly indicates the advantage of hierarchically porous structure in the synthesized nanoZIF-8@MCF composites.

4. CONCLUSION

We have developed a novel strategy for the synthesis of hierarchical microporous ZIF-8/mesoporous MCF composites. XRD, ^{13}C NMR, N_2 sorption analysis, SEM, and TEM observation provided evidence for the successful formation of such a hierarchical structure, and the TGA measurements confirmed the good thermal stability of the hybrids. The methodology proposed in this study could be extended to grow various zeolitic imidazolate frameworks, e.g., variety in pore sizes or in functionalities, on the surface on mesoporous silica or nonsiliceous materials exhibiting amino groups. For practical applications, the pervaporation of the nanoZIF-8@MCF/PVA mixed-matrix membrane for the liquid mixture of water/ethanol showed greater separation factor and flux than most PVA-based membranes, indicating the superior properties of the synthesized nanoZIF-8/MCF composite with a hierarchical porous structure. We expect that the micro/mesoporous ZIF-8/MCF composites can potentially be further applied in many fields such as molecular sorption, separation, and catalysis of large organic molecules.

■ ASSOCIATED CONTENT

Ⓢ Supporting Information

^{13}C CPMAS NMR, IR spectra, N_2 adsorption/desorption isotherms, pore size distribution, and thermal gravimetric analysis (TGA) profiles of the synthesized materials. This material is available free of charge via the Internet at http://pubs.acs.org.

■ AUTHOR INFORMATION

Corresponding Authors

*E-mail: kevinwu@ntu.edu.tw.
*E-mail: fshieh@ncu.edu.tw.

Notes

The authors declare no competing financial interest.

■ ACKNOWLEDGMENTS

K. C.-W. Wu and Fa-Kuen Shieh would like to thank the following agencies for funding: National Science Council of Taiwan (101-2628-E-002-015-MY3, 101-2923-E-002-012-MY3, 102-2113-M008-001, and 103-2118-E-002-010), National Taiwan University (102R7842 and 102R7740), Center of Strategic Materials Alliance for Research and Technology (SMART Center), and National Taiwan University (102R104100), as well as the special financial support of the Aim for Top University Project by the Ministry of Education, Taiwan.

■ REFERENCES

(1) Valtchev, V.; Tosheva, L. Porous Nanosized Particles: Preparation, Properties, and Applications. *Chem. Rev.* **2013**, *113* (8), 6734−6760.

(2) Christensen, C. H.; Johannsen, K.; Schmidt, I.; Christensen, C. H. Catalytic Benzene Alkylation over Mesoporous Zeolite Single Crystals: Improving Activity and Selectivity with a New Family of Porous Materials. *J. Am. Chem. Soc.* **2003**, *125* (44), 13370−13371.

(3) Lin, Y.; Li, Z.; Chen, Z.; Ren, J.; Qu, X. Mesoporous Silica-Encapsulated Gold Nanoparticles as Artificial Enzymes for Self-Activated Cascade Catalysis. *Biomaterials* **2013**, *34* (11), 2600−2610.

(4) Alkordi, M. H.; Liu, Y.; Larsen, R. W.; Eubank, J. F.; Eddaoudi, M. Zeolite-Like Metal−Organic Frameworks as Platforms for Applications: On Metalloporphyrin-Based Catalysts. *J. Am. Chem. Soc.* **2008**, *130* (38), 12639−12641.

(5) Yang, Z.; Xia, Y.; Mokaya, R. Enhanced Hydrogen Storage Capacity of High Surface Area Zeolite-Like Carbon Materials. *J. Am. Chem. Soc.* **2007**, *129* (6), 1673−1679.

(6) Everett, D. H. Definitions, Terminology and Symbols in Colloid and Surface Chemistry. *Pure Appl. Chem.* **1972**, *31* (4), 577.

(7) Ming, H.; Torad, N. L. K.; Chiang, Y.-D.; Wu, K. C. W.; Yamauchi, Y. Size- and Shape-Controlled Synthesis of Prussian Blue Nanoparticles by a Polyvinylpyrrolidone-Assisted Crystallization Process. *CrystEngComm* **2012**, *14* (10), 3387−3396.

(8) Hu, M.; Belik, A. A.; Imura, M.; Mibu, K.; Tsujimoto, Y.; Yamauchi, Y. Synthesis of Superparamagnetic Nanoporous Iron Oxide Particles with Hollow Interiors by Using Prussian Blue Coordination Polymers. *Chem. Mater.* **2012**, *24* (14), 2698−2707.

(9) Hayashi, H.; Cote, A. P.; Furukawa, H.; O'Keeffe, M.; Yaghi, O. M. Zeolite A Imidazolate Frameworks. *Nat. Mater.* **2007**, *6* (7), 501−506.
(10) Morris, W.; Doonan, C. J.; Furukawa, H.; Banerjee, R.; Yaghi, O. M. Crystals as Molecules: Postsynthesis Covalent Functionalization of Zeolitic Imidazolate Frameworks. *J. Am. Chem. Soc.* **2008**, *130* (38), 12626−12627.
(11) Wang, B.; Cote, A. P.; Furukawa, H.; O'Keeffe, M.; Yaghi, O. M. Colossal Cages in Zeolitic Imidazolate Frameworks as Selective Carbon Dioxide Reservoirs. *Nature* **2008**, *453* (7192), 207−211.
(12) Phan, A.; Doonan, C. J.; Uribe-Romo, F. J.; Knobler, C. B.; O'Keeffe, M.; Yaghi, O. M. Synthesis, Structure, and Carbon Dioxide Capture Properties of Zeolitic Imidazolate Frameworks. *Acc. Chem. Res.* **2009**, *43* (1), 58−67.
(13) Shi, G. M.; Yang, T.; Chung, T. S. Polybenzimidazole (PBI)/Zeolitic Imidazolate Frameworks (ZIF-8) Mixed Matrix Membranes for Pervaporation Dehydration of Alcohols. *J. Membr. Sci.* **2012**, *415*−*416* (0), 577−586.
(14) Liu, X.; Jin, H.; Li, Y.; Bux, H.; Hu, Z.; Ban, Y.; Yang, W. Metal−Organic Framework ZIF-8 Nanocomposite Membrane for Efficient Recovery of Furfural via Pervaporation and Vapor Permeation. *J. Membr. Sci.* **2013**, *428* (0), 498−506.
(15) Liu, S.; Liu, G.; Zhao, X.; Jin, W. Hydrophobic-ZIF-71 Filled PEBA Mixed Matrix Membranes for Recovery of Biobutanol via Pervaporation. *J. Membr. Sci.* **2013**, *446* (0), 181−188.
(16) Kang, C.-H.; Lin, Y.-F.; Huang, Y.-S.; Tung, K.-L.; Chang, K.-S.; Chen, J.-T.; Hung, W.-S.; Lee, K.-R.; Lai, J.-Y. Synthesis of ZIF-7/Chitosan Mixed-matrix Membranes with Improved Separation Performance of Water/Ethanol Mixtures. *J. Membr. Sci.* **2013**, *438* (0), 105−111.
(17) Sun, L.-B.; Li, J.-R.; Lu, W.; Gu, Z.-Y.; Luo, Z.; Zhou, H.-C. Confinement of Metal−Organic Polyhedra in Silica Nanopores. *J. Am. Chem. Soc.* **2012**, *134* (38), 15923−15928.
(18) Lopez-Orozco, S.; Inayat, A.; Schwab, A.; Selvam, T.; Schwieger, W. Zeolitic Materials with Hierarchical Porous Structures. *Adv. Mater.* **2011**, *23* (22−23), 2602−2615.
(19) Ivanova, I. I.; Knyazeva, E. E. Micro-mesoporous Materials Obtained by Zeolite Recrystallization: Synthesis, Characterization and Catalytic Applications. *Chem. Soc. Rev.* **2013**, *42*, 3671−3688.
(20) Han, Y.; Lee, S. S.; Ying, J. Y. Pressure-Driven Enzyme Entrapment in Siliceous Mesocellular Foam. *Chem. Mater.* **2006**, *18* (3), 643−649.
(21) Hua, J.; Han, Y. One-Step Preparation of Zeolite Silicalite-1 Microspheres with Adjustable Macroporosity. *Chem. Mater.* **2009**, *21* (12), 2344−2348.
(22) Yamauchi, Y. Field-Induced Alignment Controls of One-Dimensional Mesochannels in Mesoporous Materials. *J. Ceram. Soc. Jpn.* **2013**, *121* (1417), 831−840.
(23) Fu, Y.-Y.; Yang, C.-X.; Yan, X.-P. Fabrication of ZIF-8@SiO2 Core−Shell Microspheres as the Stationary Phase for High-Performance Liquid Chromatography. *Chem.—Eur. J.* **2013**, *19* (40), 13484−13491.
(24) Shekhah, O.; Fu, L.; Sougrat, R.; Belmabkhout, Y.; Cairns, A. J.; Giannelis, E. P.; Eddaoudi, M. Successful Implementation of the Stepwise Layer-by-Layer Growth of MOF Thin Films on Confined Surfaces: Mesoporous Silica Foam as a First Case Study. *Chem. Commun.* **2012**, *48* (93), 11434−11436.
(25) Vivero-Escoto, J. L.; Chiang, Y.-D.; Wu, K. C.-W.; Yamauchi, Y. Recent Progress in Mesoporous Titania Materials: Adjusting Morphology for Innovative Applications. *Sci. Technol. Adv. Mater.* **2012**, *13*, 013003.
(26) Sorribas, S.; Zornoza, B.; Tellez, C.; Coronas, J. Ordered Mesoporous Silica-(ZIF-8) Core-Shell Spheres. *Chem. Commun.* **2012**, *48* (75), 9388−9390.
(27) Shin, Y.; Liu, J.; Wang, L.-Q.; Nie, Z.; Samuels, W. D.; Fryxell, G. E.; Exarhos, G. J. Ordered Hierarchical Porous Materials: Towards Tunable Size- and Shape-Selective Microcavities in Nanoporous Channels. *Angew. Chem., Int. Ed.* **2000**, *39* (15), 2702−2707.
(28) Davis, M. E. Ordered Porous Materials for Emerging Applications. *Nature* **2002**, *417* (6891), 813−821.
(29) Valtchev, V.; Smaihi, M.; Faust, A.-C.; Vidal, L. Biomineral-Silica-Induced Zeolitization of Equisetum Arvense. *Angew. Chem., Int. Ed.* **2003**, *42* (24), 2782−2785.
(30) El-Nafaty, U. A.; Mann, R. Support-Pore Architecture Optimization in FCC Catalyst Particles Using Designed Pore Networks. *Chem. Eng. Sci.* **1999**, *54* (15−16), 3475−3484.
(31) Schmidt-Winkel, P.; Lukens, W. W.; Zhao, D.; Yang, P.; Chmelka, B. F.; Stucky, G. D. Mesocellular Siliceous Foams with Uniformly Sized Cells and Windows. *J. Am. Chem. Soc.* **1998**, *121* (1), 254−255.
(32) Zhao, D.; Feng, J.; Huo, Q.; Melosh, N.; Fredrickson, G. H.; Chmelka, B. F.; Stucky, G. D. Triblock Copolymer Syntheses of Mesoporous Silica with Periodic 50 to 300 Angstrom Pores. *Science* **1998**, *279* (5350), 548−552.
(33) Zhao, D.; Huo, Q.; Feng, J.; Chmelka, B. F.; Stucky, G. D. Nonionic Triblock and Star Diblock Copolymer and Oligomeric Surfactant Syntheses of Highly Ordered, Hydrothermally Stable, Mesoporous Silica Structures. *J. Am. Chem. Soc.* **1998**, *120* (24), 6024−6036.
(34) He, Q.; Shi, J.; Cui, X.; Zhao, J.; Chen, Y.; Zhou, J. Rhodamine B-Co-Condensed Spherical SBA-15 Nanoparticles: Facile Co-Condensation Synthesis and Excellent Fluorescence Features. *J. Mater. Chem.* **2009**, *19* (21), 3395−3403.
(35) Huang, A.; Dou, W.; Caro, J. Steam-Stable Zeolitic Imidazolate Framework ZIF-90 Membrane with Hydrogen Selectivity Through Covalent Functionalization. *J. Am. Chem. Soc.* **2010**, *132* (44), 15562−15564.
(36) Park, K. S.; Ni, Z.; Côté, A. P.; Choi, J. Y.; Huang, R.; Uribe-Romo, F. J.; Chae, H. K.; O'Keeffe, M.; Yaghi, O. M. Exceptional Chemical and Thermal Stability of Zeolitic Imidazolate Frameworks. *Proc. Natl. Acad. Sci.* **2006**, *103* (27), 10186−10191.
(37) Pan, Y.; Liu, Y.; Zeng, G.; Zhao, L.; Lai, Z. Rapid Synthesis of Zeolitic Imidazolate Framework-8 (ZIF-8) Nanocrystals in an Aqueous System. *Chem. Commun.* **2011**, *47* (7), 2071−2073.
(38) Teng, M.-Y.; Lee, K.-R.; Fan, S.-C.; Liaw, D.-J.; Huang, J.; Lai, J.-Y. Development of Aromatic Polyamide Membranes for Pervaporation and Vapor Permeation. *J. Membr. Sci.* **2000**, *164* (1−2), 241−249.
(39) Zhan, W.-w.; Kuang, Q.; Zhou, J.-z.; Kong, X.-j.; Xie, Z.-x.; Zheng, L.-s. Semiconductor@Metal−Organic Framework Core−Shell Heterostructures: A Case of ZnO@ZIF-8 Nanorods with Selective Photoelectrochemical Response. *J. Am. Chem. Soc.* **2013**, *135* (5), 1926−1933.
(40) Tanev, P. T.; Pinnavaia, T. J. A Neutral Templating Route to Mesoporous Molecular Sieves. *Science* **1995**, *267* (5199), 865−867.
(41) Han, Y.; Lee, S. S.; Ying, J. Y. Spherical Siliceous Mesocellular Foam Particles for High-Speed Size Exclusion Chromatography. *Chem. Mater.* **2007**, *19* (9), 2292−2298.
(42) Schmidt-Winkel, P.; Lukens, W. W.; Yang, P.; Margolese, D. I.; Lettow, J. S.; Ying, J. Y.; Stucky, G. D. Microemulsion Templating of Siliceous Mesostructured Cellular Foams with Well-Defined Ultralarge Mesopores. *Chem. Mater.* **2000**, *12* (3), 686−696.
(43) Liang, L.; Ruckenstein, E. Polyvinyl Alcohol-Polyacrylamide Interpenetrating Polymer Network Membranes and Their Pervaporation Characteristics for Ethanol-Water Mixtures. *J. Membr. Sci.* **1995**, *106* (1−2), 167−182.
(44) Ruckenstein, E.; Liang, L. Poly(acrylic acid)−poly(vinyl alcohol) Semi- and Interpenetrating Polymer Network Pervaporation Membranes. *J. Appl. Polym. Sci.* **1996**, *62* (7), 973−987.
(45) Gao, Z.; Yue, Y.; Li, W. Application of Zeolite-Filled Pervaporation Membrane. *Zeolites* **1996**, *16* (1), 70−74.
(46) Chiang, W.-Y.; Lin, Y.-H. Properties of Modified Poly(vinyl alcohol) Membranes Prepared by the Grafting of New Polyelectrolyte Copolymers for Water−Ethanol Mixture Separation. *J. Appl. Polym. Sci.* **2002**, *86* (11), 2854−2859.
(47) Yeh, J.-M.; Yu, M.-Y.; Liou, S.-J. Dehydration of Water−Alcohol Mixtures by Vapor Permeation Through PVA/Clay Nanocomposite Membrane. *J. Appl. Polym. Sci.* **2003**, *89* (13), 3632−3638.

(48) Rafik, M.; Mas, A.; Guimon, M. F.; Guimon, C.; Elharfi, A.; Schué, F. Plasma-Modified Poly(vinyl alcohol) Membranes for the Dehydration of Ethanol. *Polym. Int.* **2003**, *52* (7), 1222−1229.
(49) Ye, L. Y.; Liu, Q. L.; Zhang, Q. G.; Zhu, A. M.; Zhou, G. B. Pervaporation Characteristics and Structure of Poly(vinyl alcohol)/Poly(ethylene glycol)/Tetraethoxysilane Hybrid Membranes. *J. Appl. Polym. Sci.* **2007**, *105* (6), 3640−3648.
(50) Gimenes, M. L.; Liu, L.; Feng, X. Sericin/Poly(vinyl alcohol) Blend Membranes for Pervaporation Separation of Ethanol/Water Mixtures. *J. Membr. Sci.* **2007**, *295* (1−2), 71−79.
(51) Zhang, Q. G.; Liu, Q. L.; Chen, Y.; Chen, J. H. Dehydration of Isopropanol by Novel Poly(vinyl alcohol)−Silicone Hybrid Membranes. *Ind. Eng. Chem. Res.* **2007**, *46* (3), 913−920.